Structural, electronic, and magnetic properties of 13-, 55-, and 147-atom clusters of Fe, Co, and Ni: A spin-polarized density functional study

Ranber Singh*
Institut für Anorganische Chemie, RWTH, D-52056 Aachen, Germany

Peter Kroll
Department of Chemistry and Biochemistry, University of Texas, Arlington, Texas 76019, USA
(Received 25 August 2008; revised manuscript received 15 October 2008; published 3 December 2008)

Atomic clusters of 13, 55, and 147 atoms of Fe, Co, and Ni with several values of total magnetic moments were scanned, and minimum of total energy with respect to the total magnetic moment was searched using *ab initio* calculations based on spin-polarized density functional theory. After complete structural relaxation the icosahedral and cuboctahedral clusters retain their initial structural symmetry. However, anticuboctahedral Fe_{13}, after complete structural relaxation, adopted bcc-like structure while anticuboctahedral Co_{13} and Ni_{13} finally adopted C_{2V} symmetry. It was found that icosahedral structures are lower in energy than octahedral structures at all total magnetic moments. The cohesive energy and nearest-neighbor interatomic distance increase toward the bulk value as size of the cluster is increased. The electronic and magnetic structures of a cluster are sensitive to interatomic distance, size, and geometrical symmetry of the cluster. The local magnetic moment of surface atom increases almost linearly while local magnetic moment of center atom increases nonmonotonically as total magnetic moment of cluster is increased. The M_{13} and M_{55} (M=Fe, Co, Ni) atomic clusters are half metallic in the sense that highest occupied molecular orbital-lowest unoccupied molecular orbital (HOMO-LUMO) energy gap is very small for minority spin as compared to that for majority-spin component. However, 147-atom clusters are metallic as the HOMO-LUMO energy gap for both spin components is zero or nearly zero.

DOI: 10.1103/PhysRevB.78.245404 PACS number(s): 36.40.Cg, 71.15.Mb, 71.15.Pd, 74.25.Jb

I. INTRODUCTION

The atomic clusters are envisioned as playing a crucial role in a number of industrial applications such as catalysis, electronics, and optics.[1–4] They can be used as building blocks ("superatoms") to synthesize new materials with tailor-made properties.[5–7] The study of atomic clusters has, thus, attracted attention due to the fundamental importance of understanding the properties of materials as their size increases from atomic to molecular and supermolecular to bulk length scale. Experimental techniques for a selective production and analysis of atomic clusters have improved dramatically over the last years providing data about their physical and structural properties for comparison with theoretical calculations. This has created an intense interest in the theoretical study of atomic clusters using computer simulation techniques.[8,9] The first three closed-shell icosahedral and cuboctahedral clusters occur for 13, 55, and 147 atoms. The closed-shell atomic clusters at size of 147 atoms are observed to have unique characteristics.[10–13] Parks *et al.*[14] through chemical reaction probes of metal clusters with $H_2(D_2)$, H_2O, NH_3, and N_2 showed that bare and hydrogenated 147-atom Ni clusters have nonicosahedral structures. But when heated from 20 to 85 °C there occurs a phase transition from nonicosahedral to icosahedral structure. Recently, Teng *et al.*[15] using molecular-dynamics simulations showed there occurs surface melting in Ni_{147} clusters while in smaller clusters there occurs direct melting or glass transition. Magnetic moment decreases significantly in 4*d* transition-metal (Ru, Rh, Pd) clusters above 147 atoms.[16,17]

Atomic clusters are not just small pieces of corresponding bulk materials. Rather their structural, electronic, optical, and magnetic properties are remarkably size dependent with a quite typical nonlinear behavior[8,9,18] with increasing size of the cluster. In particular, ferromagnetic transition-metal clusters of Fe, Co, and Ni are attracting great interest for long time because of their fascinating magnetic properties which depend on their intrastructure and size.[18,19] In the bulk phase, Fe, Co, and Ni form a special class of ferromagnetic materials or compounds among the transition-metal elements. Small clusters of these elements have shown astonishing properties: they exhibit strongly enhanced magnetic moments in comparison to their corresponding bulk phase.[20–22] This effect is attributed to the reduced coordination of atoms at the surface of cluster. Several experimental reports showed magnetic properties of these clusters ranging from ferromagnetism to superparamagnetism.[18,19,23–25] Experimental observations also show an oscillatory nonmonotonic decrease in magnetic moment with increasing size of the cluster. These oscillatory changes occur close to clusters with a magic number of atoms, which correspond to completed shell icosahedrons. As these experimental techniques do not give any information about atomic arrangement of atoms, chemical reactions with ammonia as well as photoionization experiments have been used to obtain clues for the geometrical structures of Fe, Co, and Ni clusters.[26] These experiments provided strong evidences for polyicosahedral structures in small Fe, Co, and Ni clusters. Some theoretical works has been done to understand the evolution of magnetism with increasing size as well as the dependence of magnetism on size and intrastructure in Fe, Co, and Ni clusters with different geometries.[27–34] Calculations show that icosahedral clusters typically exhibit higher magnetic moment than other

 ©2008 The American Physical Society

clusters of same size. Billas *et al.*[18] applied a magnetic shell model to explain the oscillatory magnetic moment behavior with increasing size of cluster. This model predicts properties of small magnetic clusters which are partially in agreement with experimental observations. An oversimplified assumption made in this shell model is that clusters are structureless and formed by several atomic shells with no variation in magnetic moment per atom of each shell as the cluster size changes. There are still many issues which provide motivation for more extensive studies on these clusters with reasonably accurate computational techniques. In recent publications, authors also studied transition-metal clusters with structures different from icosahedral and cuboctahedral.[35–37] Surprisingly, layered Co clusters have been predicted as ground-state structures.[36]

The study of magnetic clusters of Fe, Ni, and Co is important due to many reasons: (i) it is still an open question how ferromagnetism evolve in these materials with the increasing size, atom→cluster→bulk,[19] (ii) because of unusual magnetic behavior of these clusters as compared to the corresponding bulk,[18,20–22] (iii) biomedical applications such as magnetic-resonance contrast enhancement, cell and DNA separation, and drug delivery,[38–40] and (iv) these clusters embedded in an immiscible medium are speculated to be used for technical applications such as high-density magnetic recording, optical devices and sensors, etc.[41,42] In this paper we report the spin-polarized density functional calculations on electronic and magnetic structures of icosahedral and cuboctahedral clusters of 13, 55, and 147 atoms of Fe, Co, and Ni.

II. COMPUTATIONAL DETAILS

We performed *ab initio* geometry optimization of icosahedral (ico), cuboctahedral (cubo), and anticuboctahedral (anticubo) clusters of 13, 55, and 147 atoms of Fe, Co, and Ni using the spin-polarized density functional theory (DFT) and the generalized gradient approximation (GGA) (Ref. 43) as implemented in Vienna *ab initio* simulation package (VASP).[44,45] The calculations are performed keeping the total difference between spin-up and spin-down electrons fixed. Atomic clusters with several values of total magnetic moments are scanned and minimum of total energy with respect to the total magnetic moment is searched. Furthermore, we assume a collinear spin configuration. We employed standard projector augmented wave (PAW) pseudopotentials.[46,47] The electronic configuration considered is $3d^7 4s^1$ for Fe atoms, $3d^8 4s^1$ for Co atoms, and $3d^9 4s^1$ for Ni atoms. The inclusion of inner-shell p electrons has also been tested but it did not affect results significantly. We used kinetic-energy cutoff of 270 eV. Tests using 400 eV showed no significant differences. Our choice of pseudopotentials gives correct ground-state structures for bulk phases of Fe, Co, and Ni. In Table I we list the results of reference calculations for Fe, Co, and Ni in bcc, hcp, and fcc structures. In contrast to bulk calculations for which we used Monkhorst-Pack grids, we perform cluster calculations using Γ point only. The clusters are initialized with equal bond lengths throughout and then optimized. No symmetry constraints were imposed on the structural geometry of clusters during structural relaxation. The structural optimization was performed using the conjugate gradient optimization as implemented in VASP. The structures are optimized until the atomic forces are converged to better than 0.01 eV/Å. For the analysis of local magnetic structure of clusters, we used the default values of Wigner-Seitz radii of atoms as provided in VASP. As a consequence, the sum of local atomic magnetic moments computed around each atom is not exactly equal to the overall total magnetic moment of a cluster but it does not affect the energy of the cluster and its electronic and magnetic properties. We used a cubic simulation box for the relaxation of isolated freestanding clusters. The simulation boxes have lattice parameters of 15 Å for 13-atom, 20 Å for 55-atom, and 22 Å for 147-atom clusters. These simulation boxes have been tested for negligible interaction between a cluster and its images.

TABLE I. Nearest-neighbor interatomic distance, energy per atom, and magnetic moment in bcc, fcc, and hcp structures of Fe, Co, and Ni. These structures are optimized using PAW pseudopotentials and energy cutoff of 270 eV. It correctly predicts the ground-state structures (Ref. 49): bcc for Fe, hcp for Co, and fcc for Ni.

	Structure	Nearest-neighbor interatomic distance (Å)	Energy (eV/atom)	Magnetic moment (μ_B/atom)
Fe	bcc	2.43	−8.162	2.13
	fcc	2.43	−8.066	0.43
	hcp	2.45	−8.143	0.06
Co	bcc	2.42	−6.875	1.70
	fcc	2.43	−6.820	0.16
	hcp	2.48	−6.986	1.59
Ni	bcc	2.41	−5.364	0.50
	fcc	2.48	−5.453	0.65
	hcp	2.47	−5.432	0.64

III. RESULTS AND DISCUSSION

A. 13-atom clusters

1. Fe_{13} clusters

We computed Fe_{13} clusters with a total magnetic moment ranging from $32\mu_B$ to $45\mu_B$ in icosahedral, cuboctahedral, and anticuboctahedral structural symmetries. The results are given in Table II and Figs. 2 and 3. In Fig. 2 we plot the total energy of the cluster as a function of its total magnetic moment while in Fig. 3 the magnetic profile of a cluster in terms of local magnetic moments of center and surface atoms as a function of the total magnetic moment of a cluster. Figure 2 shows that ico-Fe_{13} clusters are about 2.0 eV lower in energy than cubo-Fe_{13} clusters and about 1.0 eV lower than anticubo-Fe_{13} clusters for each magnetic moment. Figure 2 indicates two local minima for both ico-Fe_{13} and cubo-Fe_{13} clusters: a low-spin (ls) state and a high-spin (hs) state. The low-spin state of ico-Fe_{13} with a total magnetic moment of $34\mu_B$ exhibits antiferromagnetic (AFM) ordering and an interatomic Fe-Fe distance of 2.35 Å between central Fe and

TABLE II. Total magnetic moment, energy per atom, interatomic distance between center atom, and surface atoms in the ground-state ls and hs atomic clusters of 13 atoms of Fe, Co, and Ni. The energy differences (ΔE) between ground states of icosahedral, cuboctahedral, and anticuboctahedral relative to global minimum structure are also given in the table. AFM stands for antiferromagnetic and FM for ferromagnetic coupling between center atom and surrounding atoms. The aiMD clusters are Fe_{13} clusters optimized using *ab initio* molecular-dynamics simulations.

		Magnetic moment (μ_B)	Spin state	Interatomic distance (Å)	Energy (eV/atom)	ΔE (eV/atom)
Fe_{13}	ls-ico	34	AFM	2.35	−6.457	+0.014
	hs-ico	44	FM	2.39	−6.464	+0.007
	ls-aiMD	34	AFM	2.35	−6.458	+0.013
	hs-aiMD	44	FM	2.41	−6.471	0.000
	ls-cubo	34	AFM	2.40	−6.298	+0.173
	hs-cubo	40	FM	2.43	−6.307	+0.164
	anticubo	40	FM	2.37	−6.380	+0.091
Co_{13}	ls-ico	21	FM	2.30	−5.129	0.000
	hs-ico	31	FM	2.33	−5.122	+0.007
	ls-cubo	21	FM	2.33	−5.099	+0.030
	hs-cubo	27	FM	2.35	−5.111	+0.018
	anticubo	21	FM	2.30, 2.38[a]	−5.119	+0.010
Ni_{13}	Ico	8	FM	2.32	−3.841	0.000
	cubo	6	AFM	2.36	−3.748	+0.093
	anticubo	8	AFM	2.36, 2.37[a]	−3.777	+0.064

[a]See Fig. 1.

its 12 equidistant neighbors. The high-spin state of ico-Fe_{13} with a total magnetic moment of $44\mu_B$ exhibits ferromagnetic (FM) ordering and an interatomic Fe-Fe distance of 2.39 Å. The high-spin state is 0.09 eV (about 7 meV/atom) lower in energy as compared to low-spin state. For cubo-Fe_{13}, the low-spin state with a total magnetic moment of $34\mu_B$ exhibits AFM ordering and interatomic distance of 2.40 Å while the high-spin state with a total magnetic moment of $40\mu_B$ exhibits FM ordering and an interatomic distance of 2.43 Å between center atom and surrounding surface atoms. Here as well, the high-spin state comes out being about 0.12 eV lower in energy than the low-spin state. For anticubo Fe_{13} cluster, we found the lowest energy structure with a magnetic moment of $40\mu_B$ and FM ordering. However, Fe_{13} clusters with anticuboctahedral structure symmetry are far from being stable. After relaxation they adopt a bcc-like structure having C_{2V} point symmetry (see Fig. 1). The lowest energy relaxed Fe_{13} with total magnetic moment of $40\mu_B$ exhibits FM coupling between center atom and surrounding surface atoms.

Previous calculations by Rollmann *et al.*[48] already reported the low-spin AFM state with a total magnetic moment of $34\mu_B$ and the high-spin FM ground state with a total magnetic moment of $44\mu_B$ for ico-Fe_{13} clusters. They also pointed out that the ground-state ico-Fe_{13} cluster still exhibits a Jahn-Teller instability due to partially occupied degenerate orbitals in the minority-spin component and found a distorted icosahedral cluster with lower energy. We investigated this possibility by performing additional *ab initio* molecular-dynamics (aiMD) simulations at 300 K for about 5 ps using a time step of 0.5 fs. The spins were not restricted during the aiMD simulations. Starting with the energetically high lying cubo-Fe_{13} cluster the system readily adopted a distorted icosahedral structure. After a final quench we optimized the cluster geometry at fixed total magnetic moments similar to the procedure outlined above. We found the resulting Fe_{13} clusters having the same cluster geometry and ground-state property as proposed by Rollmann *et al.*[48] We denote these clusters as aiMD. The results for these clusters are given in Table II and Fig. 2. Figure 2 shows that similar to ideal icosahedral Fe_{13} the aiMD clusters also has two minima. The low-spin state with a total magnetic moment of $34\mu_B$ exhibits AFM ordering and an average interatomic distance of 2.35 Å between center atom and surrounding surface atoms. The high-spin state with a total magnetic moment of $44\mu_B$ exhibits FM ordering and an average interatomic distance of 2.41 Å between center atom and surrounding surface atoms. The ground state of distorted ico-Fe_{13} exhibits a pronounced energy gap between highest occupied molecular orbital (HOMO) and lowest unoccupied molecular orbital (LUMO). Upon distortion of the ideal icosahedral cluster, the degeneracy of the HOMO within the minority-spin component is lifted. The splitting is large enough to shift the HOMO of minority-spin electrons below that of majority-spin electrons. Hence, in the distorted icosahedral structure the HOMO is now within the majority-spin component. The HOMO-LUMO energy gaps for majority and minority-spin components as given in Table V show that icosahedral and cuboctahedral Fe_{13} clusters are half metallic in the sense that gap is small for minority-spin component as compared to that of majority-spin component. Considering the trend of local magnetic moments of surface atoms and center atom as a function of total magnetic moment of Fe_{13} clusters (displayed in Fig. 3), we notice that local magnetic moments of

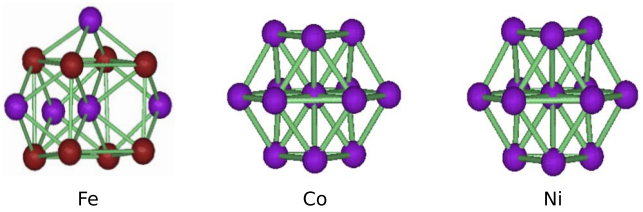

FIG. 1. (Color online) Relaxed lowest energy structures of anticuboctahedral clusters of 13 atoms of Fe, Co, and Ni. The structural optimization was performed using the conjugate gradient optimization as implemented in VASP. The initial structures of anticuboctahedral clusters were taken as ideal anticuboctahedral with the same bond length throughout. However, the relaxed Fe_{13} cluster has bcc-like structure while Co_{13} and Ni_{13} finally adopted C_{2V} symmetry. In relaxed lowest energy Co_{13} cluster atoms in the top and bottom atomic layers are at a distance of 2.30 Å and atoms in the middle atomic layer are at a distance of 2.38 Å from the center atom. In relaxed lowest energy Ni_{13} cluster atoms in the top and bottom atomic layers are at a distance of 2.36 Å and atoms in the middle atomic layer are at a distance of 2.37 Å from the center atom.

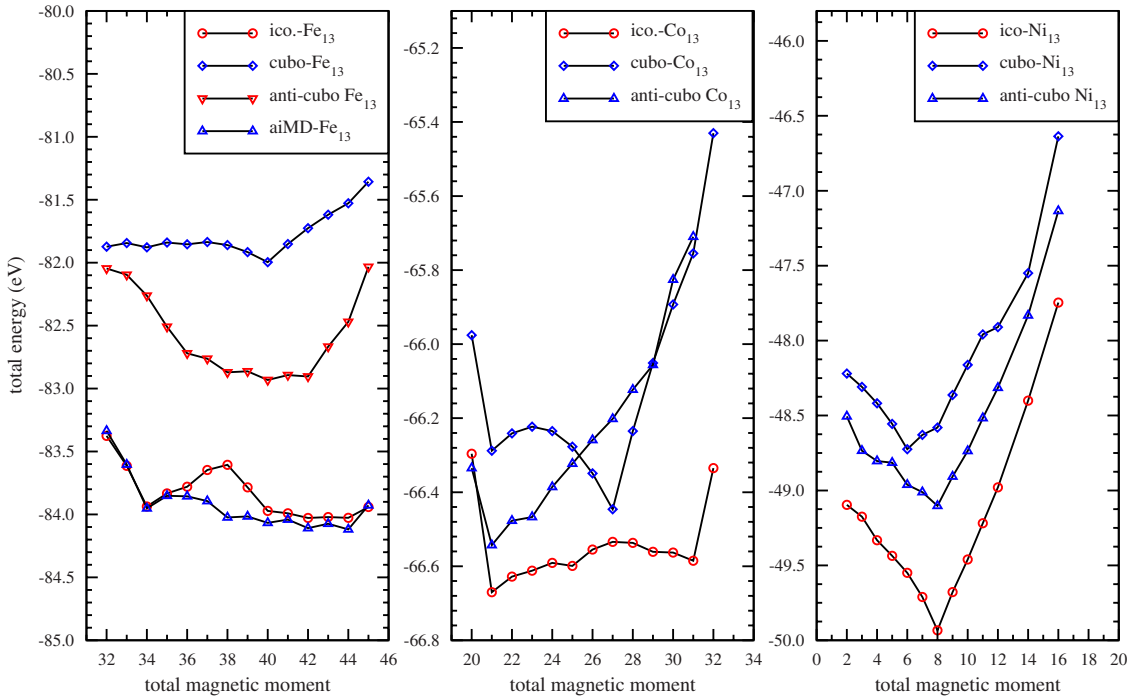

FIG. 2. (Color online) Total energy as a function of total magnetic moment in icosahedral, cuboctahedral, and anticuboctahedral clusters of 13 atoms of Fe, Co, and Ni. The aiMD-Fe_{13} clusters are Fe_{13} clusters optimized using aiMD simulations.

surface atoms are almost unaffected and are approximately equal to $2.8\mu_B$. The center atom, on the other hand, changes its spin state rather drastically. Overall the local magnetic moment of surface atom is greater than the bulk value ($2.13\mu_B$) for the total magnetic moment between $31\mu_B$ and $45\mu_B$ for all ico-Fe_{13}, cubo-Fe_{13}, and anticubo Fe_{13} clusters.

2. Co_{13} clusters

In a similar way as for Fe_{13} we studied Co_{13} clusters. We examined ico-Co_{13}, cubo-Co_{13}, and anticubo Co_{13} with a total magnetic moment ranging from $21\mu_B$ to $32\mu_B$. Total energies and magnetic profile (local magnetic moment of center and surface atoms) as a function of total magnetic moment are plotted in Figs. 2 and 4, respectively. The results for the lowest energy clusters are given in Table II. As for Fe_{13}, the energy profile of Co_{13} clusters show two local minima for both icosahedral and cuboctahedral clusters: a low-spin state and a high-spin state. In each case, however, the coupling between central and surface atoms is ferromagnetic. The low-spin state of ico-Co_{13} exhibits a total magnetic moment of $21\mu_B$ and interatomic distance of 2.30 Å. The high-spin state with total magnetic moment $31\mu_B$ has interatomic distance of 2.33 Å between center atom and surrounding surface atoms. The low spin state is lower in energy by 0.09 eV as compared to high-spin state. In a previous study Miura *et al.*[31] also reported two low energy electronic states for ico-Co_{13} clusters with total magnetic moments $23\mu_B$ and $29\mu_B$. Our attempts to optimize anticubo Co_{13} clusters always resulted in distorted geometries. Top and bottom layer atoms (see Fig. 1) come closer (2.30 Å) to the central atom while the distances to six atoms in the middle layer expand (2.38 Å) slightly. Overall the energy difference between icosahedral, cuboctahedral, and anticuboctahedral structures of Co_{13} is smaller for all magnetic moments in comparison to Fe_{13} clusters. Figure 2 shows that icosahedral clusters are always energetically favored. The lowest energy ico-Co_{13} cluster is about 0.23 eV lower relative to the lowest cubo-Co_{13} and by 0.13 eV relative to the lowest anticubo Co_{13} cluster. Previous first principles calculations[30] on Co_n ($n=4-19$) clusters have predicted that Co_{13} cluster with icosahedral symmetry has higher magnetic moment than the clusters with cuboctahedral and dodecahedral symmetries. In Fig. 4 we show the trends of the local magnetic moments of central and surface atoms as a function of total magnetic moment of the Co_{13} cluster. As expected, the local magnetic moment increases with increasing total magnetic moment of cluster. The HOMO-LUMO gaps in minority and majority-spin electron components as given in Table V show that Co_{13} clusters are half metallic in the sense that HOMO-LUMO gap for minority spins is smaller than that for majority spins.

3. Ni_{13} clusters

For Ni_{13} we studied icosahedral, cuboctahedral, and anticuboctahedral clusters with a total magnetic moment ranging from $2\mu_B$ to $16\mu_B$. The results for lowest energy Ni_{13} clusters are given in Table II. Figures 2 and 5 show total energies and magnetic profiles (local magnetic moment of center and surface atoms) as a function of total magnetic moment, respectively. Unlike Fe_{13} and Co_{13} clusters, each Ni_{13} cluster geometry (icosahedral, cuboctahedral, and anticuboctahedral) exhibits only one minimum. For ico-Ni_{13} the minimum appears at $8\mu_B$ and has FM coupling. For cubo and anticubo Ni_{13} clusters the minima have AFM coupling and appear with a total magnetic moment of $6\mu_B$ and $8\mu_B$, respectively.

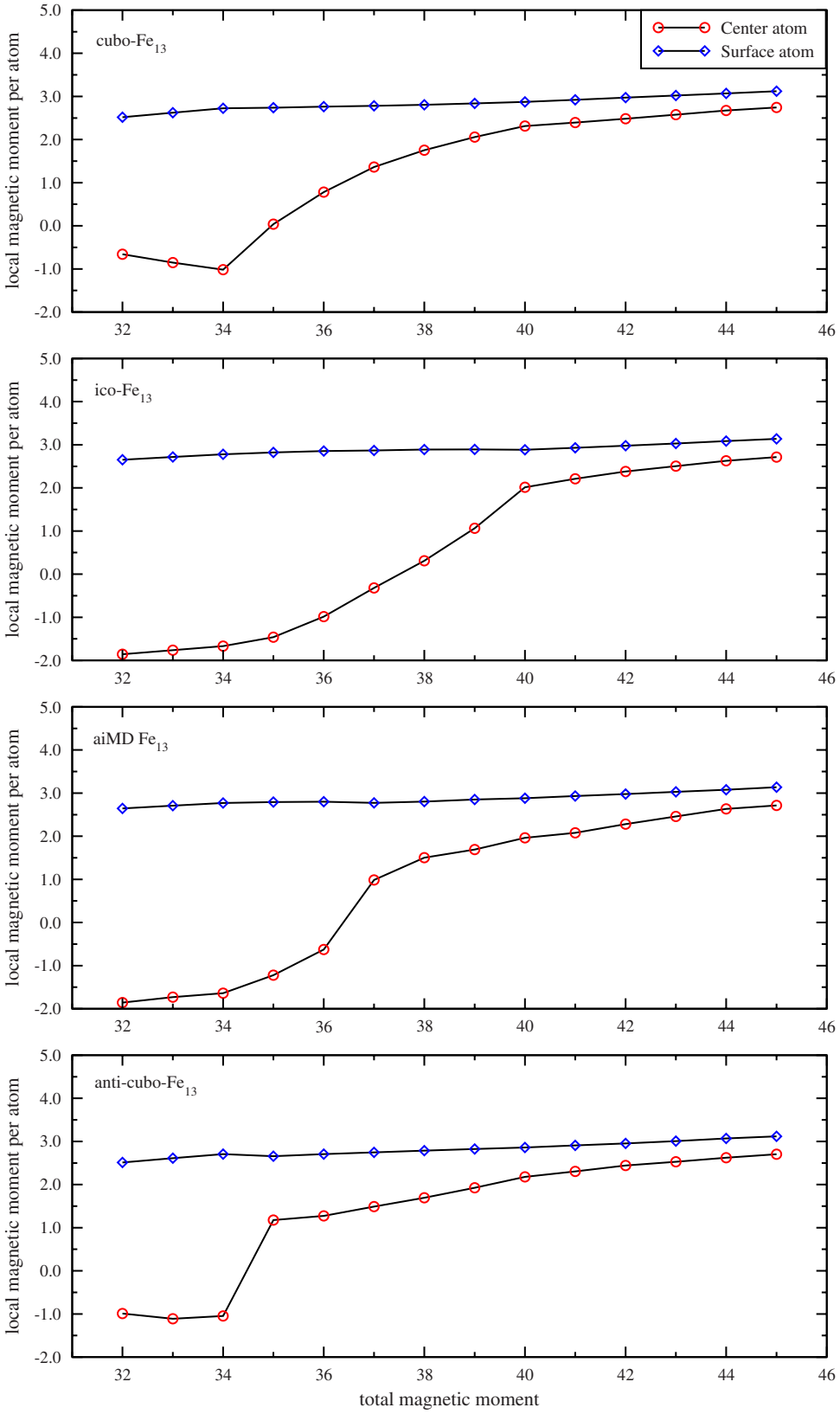

FIG. 3. (Color online) Local magnetic moment (μ_B) of center atom and surface atom in icosahedral, cuboctahedral, anticuboctahedral, and aiMD clusters of Fe_{13}.

The ico-Ni_{13} ground-state structure is clearly separated by about 1.0 eV from the anticubo Ni_{13} and 1.3 eV from the cubo-Ni_{13}. As for Co_{13}, in the lowest energy anticubo Ni_{13}, top and bottom layer atoms (see Fig. 1) come closer (2.36 Å) to the central atom while the distances to six atoms in the middle layer expand (2.37 Å) slightly. The magnetic profiles of each cluster geometry given in Fig. 5 show a crossover from FM to AFM coupling around the minimum-energy configuration. The local magnetic moment increases with increasing total magnetic moment of the cluster. The

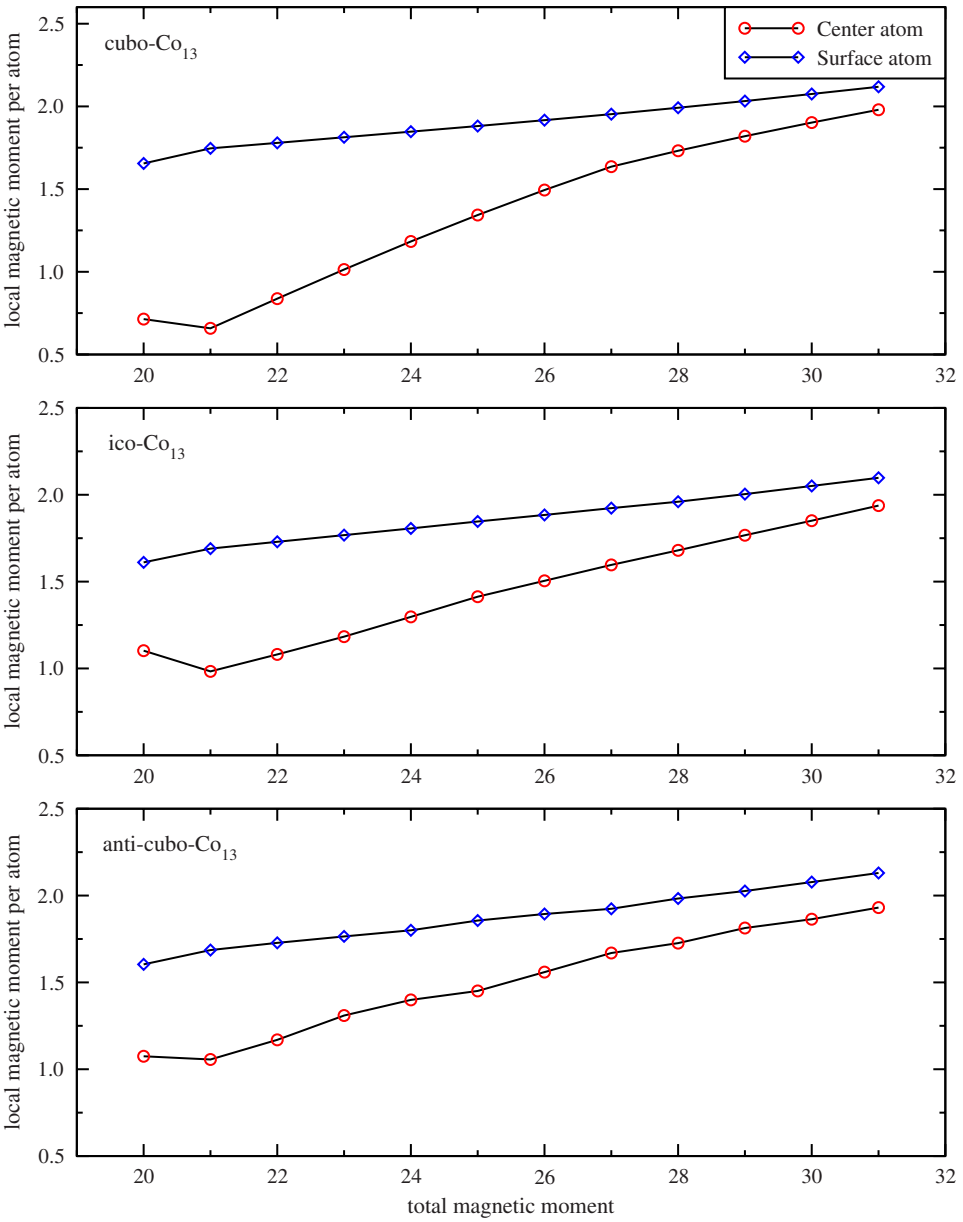

FIG. 4. (Color online) Local magnetic moment (μ_B) of center atom and surface atom in icosahedral, cuboctahedral, and anticuboctahedral clusters of Co_{13}.

HOMO-LUMO gaps in minority and majority-spin electron components are given in Table V. Similar to Fe_{13} and Co_{13} clusters the Ni_{13} clusters have HOMO-LUMO gap for minority spins smaller than that for majority spins.

B. 55-atom clusters

Our approach to investigate the 55-atom clusters of Fe, Co, and Ni was comparable to our study of the smaller 13-atom clusters. We focused on icosahedral and cuboctahedral clusters. In general, we constraint the total magnetic moment of a cluster during optimization to evaluate the energy as a function of magnetic moment. In particular, we present the local magnetic moment of the atoms in different geometric shells to study the magnetic structure in more depth.

1. Fe_{55} clusters

Clusters of Fe_{55} in icosahedral and cuboctahedral symmetries are examined for total magnetic moment ranging from $130\mu_B$ to $170\mu_B$. Total energy and magnetic profile of clusters are given in Figs. 6 and 7, respectively. As it turns out, ico-Fe_{55} clusters are preferred by about 4.0 eV (0.07 eV per atom) over cubo-Fe_{55} clusters at a given magnetic moment. The results for lowest energy clusters are given in Table III. The lowest energy cubo-Fe_{55} cluster has a total magnetic moment of $148\mu_B$ while the ground-state ico-Fe_{55} has $150\mu_B$. Both the lowest energy cubo-Fe_{55} and ico-Fe_{55} exhibit AFM coupling between the center atom and its surrounding 12 atoms in the first neighbor shell. Atoms in further geometrical shells are then ferromagnetically coupled with atoms in preceding shells. In both lowest energy structures of ico-Fe_{55} and cubo-Fe_{55} the interatomic distance between center atom and surrounding 12 neighbors in first shell is similar to the Fe-Fe bond length (2.43 Å) computed for bulk bcc Fe. However, the nearest-neighbor bond lengths between the atoms in first shell and outer shells are different in ico-Fe_{55} and cubo-Fe_{55} clusters. In ico-Fe_{55} the nearest-

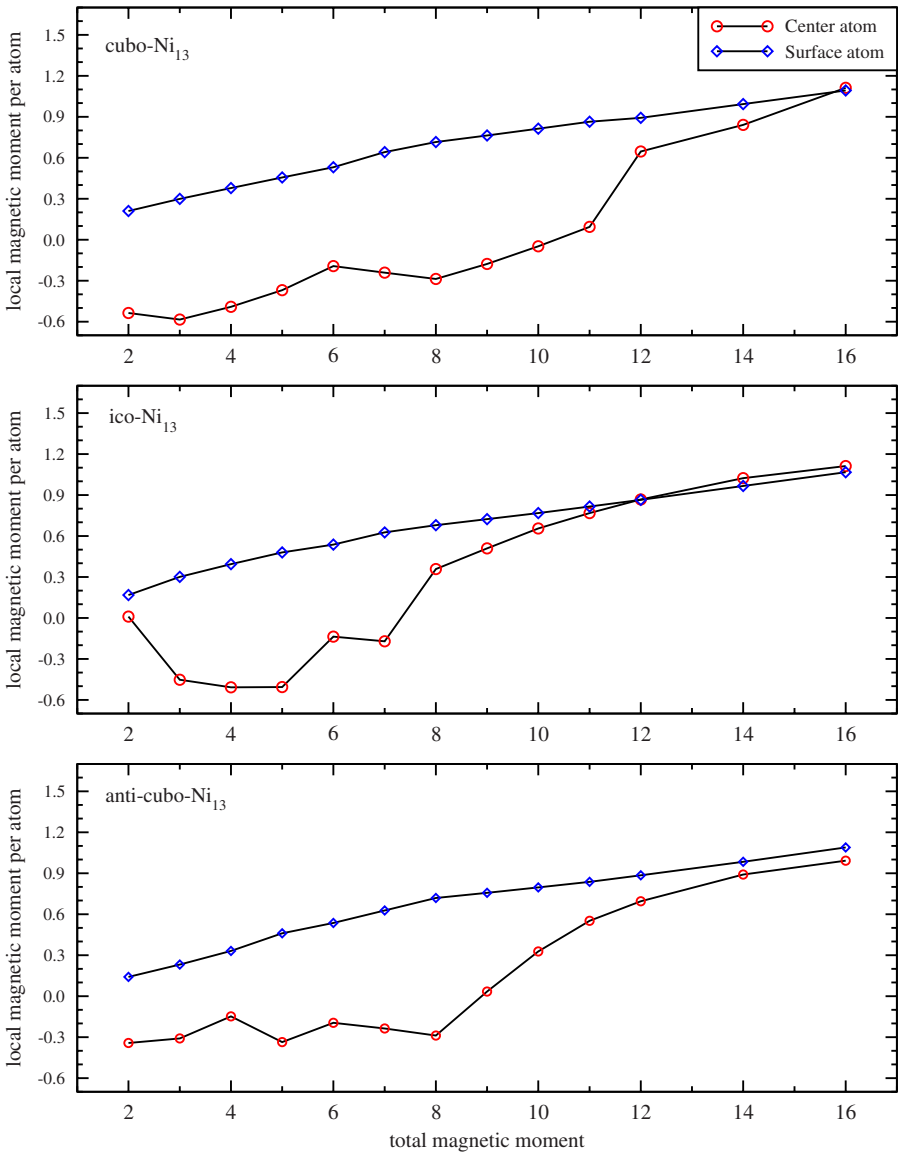

FIG. 5. (Color online) Local magnetic moment (μ_B) of center atom and surface atom in icosahedral, cuboctahedral, and anticuboctahedral clusters of Ni_{13}.

neighbor bond length between atoms in first shell is 2.45 Å and between atoms in second shell is 2.42 Å. In cubo-Fe_{55} the nearest-neighbor bond length between atoms in first shell is 2.43 Å and between atoms in second shell is 2.46 Å. Figure 7 shows the local atomic moments of the geometrical shells in Fe_{55} clusters as they develop with the total magnetic moment of the cluster. Quite similar to what has been observed for the smaller Fe_{13} cluster, it is the central atom which changes from AFM to FM coupling as the total magnetic moment of the cluster increases. The local magnetic moments in the outer geometrical shells increase almost linearly as the total magnetic moment of the cluster is increased. The outmost shells of both icosahedral and cuboctahedral clusters exhibit the largest magnetic moment, about $2.8\mu_B$, for the lowest energy structures. It is worthy to note that the AFM coupling present in the ground-state structure is lifted if total magnetic moment of the Fe_{55} cluster is slightly increased. Similar to Fe_{13} clusters the HOMO-LUMO energy gaps of Fe_{55} clusters are sensitive to the geometrical symmetry of cluster. We find that the HOMO-LUMO energy gaps for ico-Fe_{55} and cubo-Fe_{55} clusters are quite different (see Table V). Fe_{55} clusters show half metallic behavior in the sense that HOMO-LUMO energy gap for minority-spin component is small as compared to that for majority-spin component.

2. Co_{55} clusters

For Co_{55} we computed icosahedral and cuboctahedral clusters with total magnetic moments from $90\mu_B$ to $130\mu_B$. The total energies as a function of total magnetic moment are shown in Fig. 6 while the corresponding magnetic profiles are presented in Fig. 8. Figure 6 shows that ico-Co_{55} clusters are generally preferred by about 5.0 eV (0.09 eV per atom) over cubo-Co_{55} clusters for the same total magnetic moment. Around the lowest energy structure, the variation in energy with total magnetic moment is small. The results for lowest energy clusters are given in Table III. Nevertheless, we find the ground-state structure of ico-Co_{55} with $105\mu_B$. For cubo-Co_{55} we find the lowest energy configuration with $101\mu_B$. There are pronounced differences in the Co-Co distance between central atom and surrounding 12 neighbors in first shell: 2.38 Å in ico-Co_{55} and 2.48 Å in cubo-Co_{55}. In

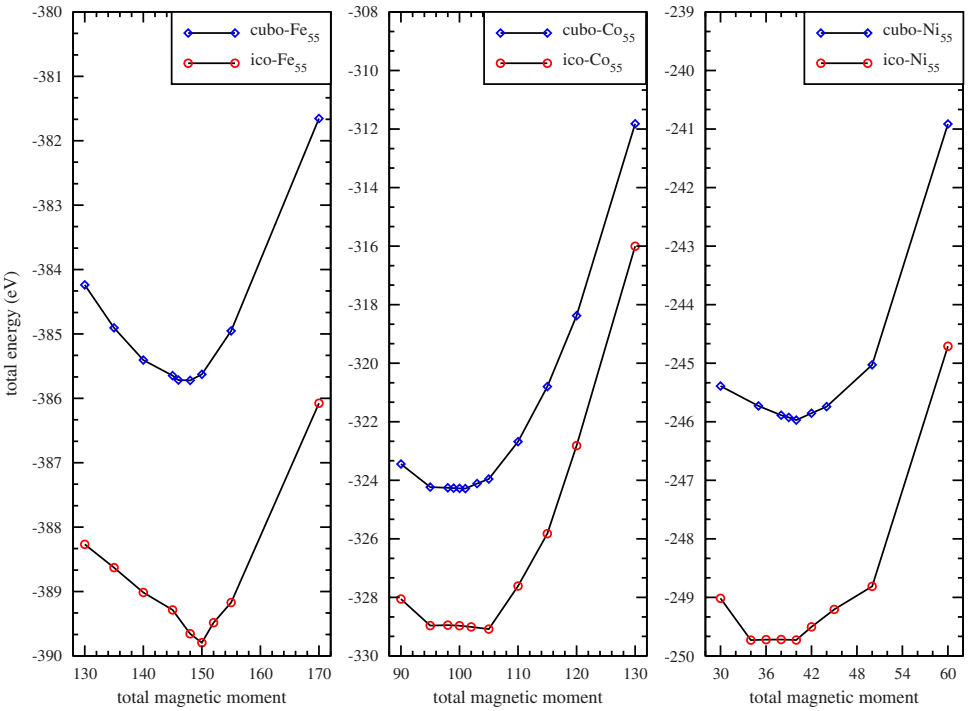

FIG. 6. (Color online) Total energy as a function of total magnetic moment in cuboctahedral and icosahedral clusters of 55 atoms of Fe, Co, and Ni.

ico-Co_{55} the nearest-neighbor bond length between atoms in first shell is 2.50 Å and between atoms in second shell is 2.37 Å. In cubo-Co_{55} the nearest-neighbor bond length between atoms in first shell is 2.48 Å and between atoms in second shell is 2.41 Å. At lowest energy both ico-Co_{55} and cubo-Co_{55} clusters exhibit FM coupling between the central atom and its surrounding atomic shells. In Fig. 8 we plot the local magnetic moment of every geometrical shell as a function of total magnetic moment of the cluster. Figure 8 shows that local magnetic moment as a function of total magnetic moment of ico-Co_{55} and cubo-Co_{55} is quite different. As for Fe_{55}, the local magnetic moments of atoms in outer shells increase almost linearly as the total magnetic moment of the cluster is increased. The HOMO-LUMO energy gaps as given in Table V show that Co_{55} clusters are half metallic in the sense that HOMO-LUMO energy gap for minority-spin component is small as compared to that for majority-spin component. Similar to Fe_{55} and 13-atom (Fe, Co, and Ni)

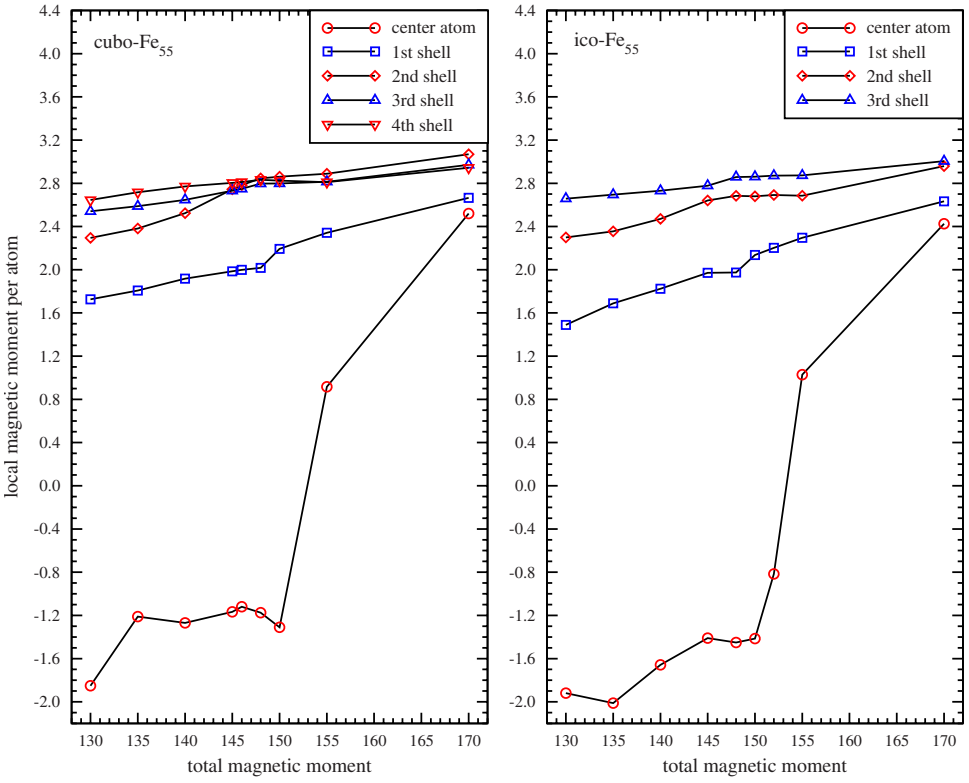

FIG. 7. (Color online) Magnetic profile of cuboctahedral and icosahedral Fe_{55} clusters. The local magnetic moment (μ_B) of atoms in spherical atomic shells around the center atom is plotted as a function of total magnetic moment of cluster.

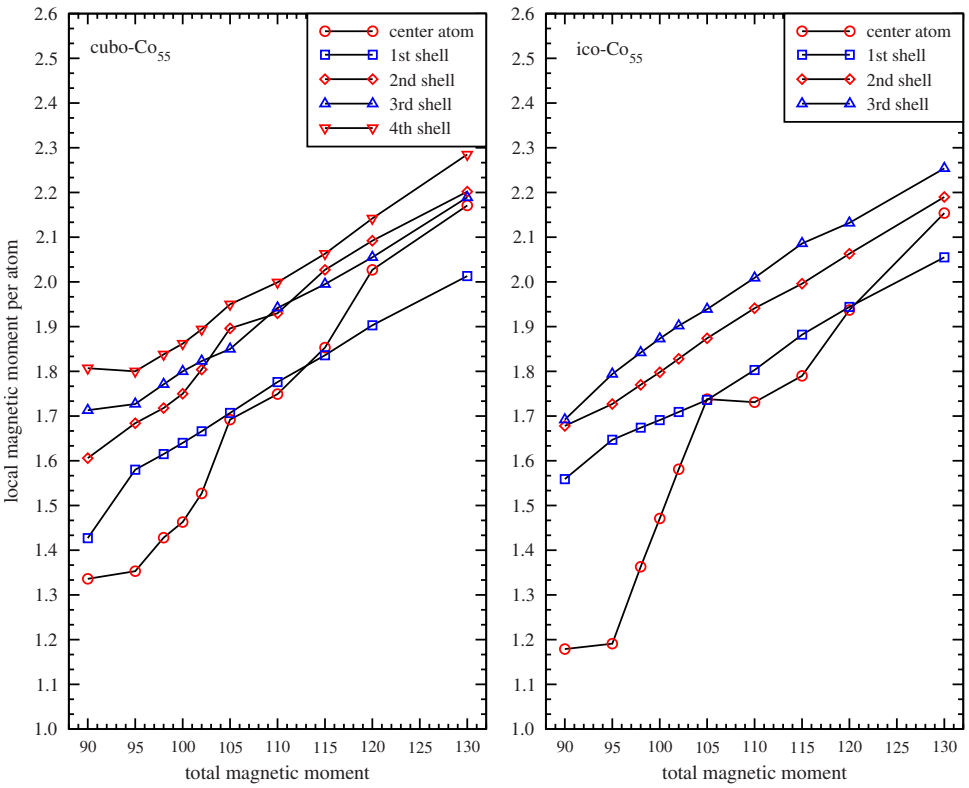

FIG. 8. (Color online) Magnetic profile of cuboctahedral and icosahedral Co_{55} clusters. The local magnetic moment (μ_B) of atoms in spherical atomic shells around the center atom is plotted as a function of total magnetic moment of cluster.

clusters the HOMO-LUMO energy gaps of Co_{55} clusters are also sensitive to the geometrical symmetry of cluster. We find that the HOMO-LUMO energy gaps for ico-Co_{55} and cubo-Co_{55} clusters are quite different (see Table V).

3. Ni_{55} clusters

Ni_{55} clusters of icosahedral and cuboctahedral symmetries were computed for a total magnetic moment from $30\mu_B$ to $60\mu_B$. Total energy and magnetic profile as a function of total magnetic moment are shown in Figs. 6 and 9, respectively. As for Fe and Co, the icosahedral clusters are preferred over cuboctahedral clusters for Ni_{55} at any total magnetic moment of the cluster. The icosahedral clusters are lower in energy by about 4 eV relative to cuboctahedral clusters for a given magnetic moment of cluster. The results for lowest energy clusters are given in Table III. The lowest energy state of cubo-Ni_{55} cluster exhibits total magnetic moment of $40\mu_B$ and an interatomic distance of 2.45 Å between center atom and surrounding 12 neighbors in first shell while the ground-state ico-Ni_{55} cluster exhibits a total magnetic moment of $40\mu_B$ and an interatomic distance of 2.35 Å between center atom and surrounding 12 neighbors in first shell. In ico-Ni_{55} the nearest-neighbor bond length between atoms in first shell is 2.47 Å and between atoms in second shell is 2.41 Å. In cubo-Ni_{55} the nearest-neighbor bond length between atoms in first shell is 2.45 Å and between atoms in second shell is 2.42 Å. Overall, the dependence of total energy on the magnetic moment is very weak. In the range from $34\mu_B$ to $40\mu_B$ all clusters have almost identical energies. It is interesting to note that in its ground-state ico-Ni_{55} has significantly shorter Ni-Ni distance in the core of the cluster in comparison to the bulk (we compute $d_{\text{Ni-Ni}}=2.48$ Å for fcc Ni). The cubo-Ni_{55} cluster comes somewhat closer to this value ($d_{\text{Ni-Ni}}=2.45$ Å). Montejano-Carrizales *et al.*[29] also reported a detailed study of structural properties of icosahedral Ni_n ($n=13$, 55, and 147) clusters using embedded-atom method. The FM coupling between all atoms is observed for both ico-Ni_{55} and cubo-Ni_{55} in their lowest energy configurations. In Fig. 9 we show local magnetic moment of atoms in the different atomic shells around the central atom as a function of total magnetic moment of the cluster. In contrast to the trends observed for Fe_{55} and Co_{55} clusters, local magnetic structure profile of Ni_{55} clusters is quite frustrated. Similar to above discussed clusters we find that Ni_{55} clusters are also

TABLE III. Total magnetic moment, nearest-neighbor interatomic distance between center atom, and 12 surrounding atoms in the ground-state atomic clusters of 55 atoms of Fe, Co, and Ni. The energy differences (ΔE) between ground states of icosahedral and cuboctahedral relative to global minimum are also given in the table. AFM stands for antiferromagnetic and FM for ferromagnetic coupling between center atom and first neighbor atoms.

	Magnetic moment (μ_B)	Spin state	Interatomic distance (Å)	Energy (eV/atom)	ΔE (eV/atom)
ico-Fe_{55}	150	AFM	2.43	−7.087	0.000
cubo-Fe_{55}	148	AFM	2.43	−7.013	+0.074
ico-Co_{55}	105	FM	2.38	−5.983	0.000
cubo-Co_{55}	101	FM	2.48	−5.896	+0.087
ico-Ni_{55}	40	FM	2.35	−4.541	0.000
cubo-Ni_{55}	40	FM	2.45	−4.472	+0.069

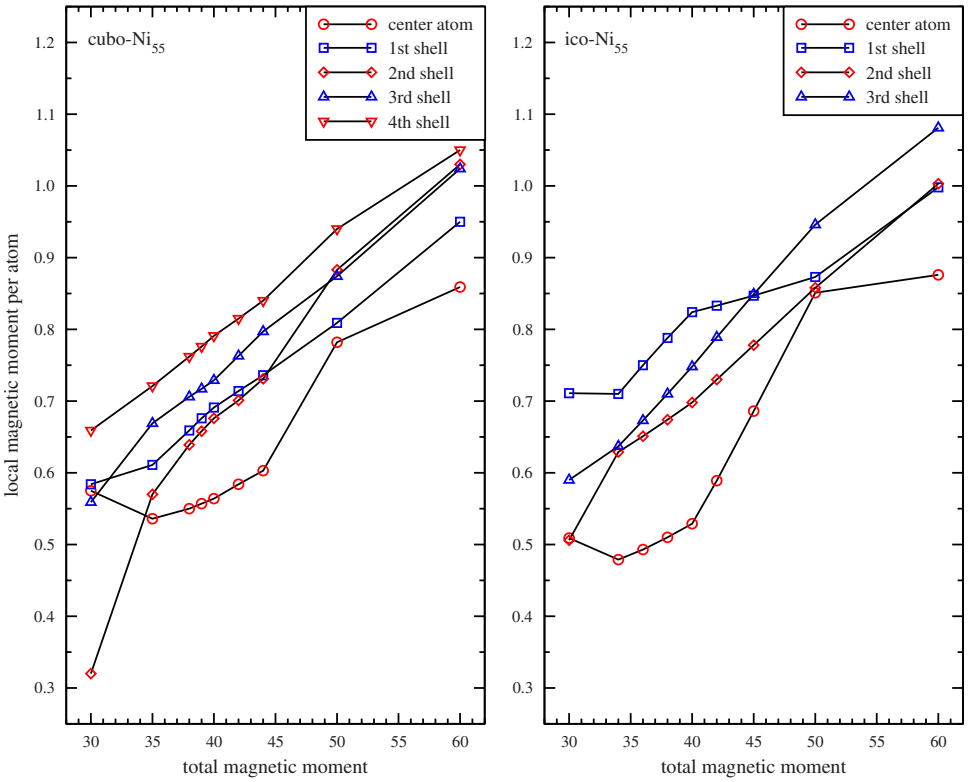

FIG. 9. (Color online) Magnetic profile of cuboctahedral and icosahedral Ni_{55} clusters. The local magnetic moment (μ_B) of atoms in spherical atomic shells around the center atom is plotted as a function of total magnetic moment of cluster.

half metallic and HOMO-LUMO energy gaps are dependent on the geometrical symmetry of cluster (see Table V).

C. 147-atom clusters

Finally we also computed similar calculations on 147-atom clusters of Fe, Co, and Ni in icosahedral and cuboctahedral structural symmetries. We find that the icosahedral clusters are still lower in energy at all total magnetic moments of the cluster. However, the energy difference between icosahedral and cuboctahedral clusters is smaller as compared to 55-atom clusters. The results for lowest energy clusters are given in Table IV. In contrast to 13- and 55-atom clusters, the lowest energy 147-atom icosahedral clusters of Fe and Co have smaller magnetic moment than cuboctahedral clusters. However, the lowest energy Ni_{147} clusters such as Ni_{55} clusters have the same magnetic moment in both icosahedral and cuboctahedral structural symmetries. The magnetic coupling between center atom and surrounding 12 atoms in the first shell in Fe_{147} clusters oscillates between AFM and FM as total magnetic moment of cluster is increased. It is AFM in lowest energy ico-Fe_{147}, whereas it is FM in lowest energy cubo-Fe_{147}. However, the 12 atoms in first atomic shell around center atom in both ico-Fe_{147} and cubo-Fe_{147} have AFM coupling with the surrounding outer atomic shells. The Co_{147} and Ni_{147} clusters in both cuboctahedral and icosahedral symmetries have FM coupling between all the atoms. Unlike half-metallic 13- and 55-atom clusters the 147-atom clusters are metallic like their bulk counterparts (see Table V) as the HOMO-LUMO energy gap for both spin components in these clusters is zero or nearly zero. Previous studies have also shown that closed-shell atomic clusters at size of 147 atoms have unique characteristics.[10–13] Recently, Teng *et al.*[15] using molecular-dynamics simulations showed there occurs surface melting in Ni_{147} clusters while in smaller clusters there occurs direct melting or glass transition. Magnetic moment decreases significantly in 4*d* transition-metal (Ru, Rh, and Pd) clusters above 147 atoms.[16,17] Thus, at this size the properties of magnetic clusters show transition toward bulk properties.

IV. CONCLUSIONS

We examined low energy atomic clusters of 13, 55, and 147 atoms of Fe, Co, and Ni by restricting the total magnetic moment. The atomic clusters with several values of total magnetic moments are scanned and minimum of total energy

TABLE IV. Total magnetic moment in the ground-state atomic clusters of 147 atoms of Fe, Co, and Ni. The energy differences (ΔE) between ground states of icosahedral and cuboctahedral relative to global minimum are also given in the table. AFM stands for antiferromagnetic and FM for ferromagnetic coupling between center atom and first neighbor atoms.

	Magnetic moment (μ_B)	Spin state	Energy (eV/atom)	ΔE (eV/atom)
ico-Fe_{147}	334	AFM	−7.329	0.000
cubo-Fe_{147}	340	FM	−7.300	+0.029
ico-Co_{147}	245	FM	−6.264	0.000
cubo-Co_{147}	255	FM	−6.194	+0.070
ico-Ni_{147}	100	FM	−4.810	0.000
cubo-Ni_{147}	100	FM	−4.765	+0.045

TABLE V. HOMO-LUMO energy gap (electron volts) in the lowest energy clusters of 13, 55, and 147 atoms of Fe, Co, and Ni. For same size of cluster the HOMO-LUMO gaps are quite different in icosahedral and cuboctahedral geometries. The M_{13} and M_{55} (M=Fe, Co, and Ni) clusters are half metallic in the sense that the gap is very small for minority-spin component as compared to majority-spin component. However, M_{147} clusters are metallic because the gaps for both spin components are zero or nearly zero.

	HOMO-LUMO energy gap (eV)					
	Icosahedral		Cuboctahedral		Anticuboctahedral	
Cluster	Majority	Minority	Majority	Minority	Majority	Minority
Fe_{13}	0.41	0.01	0.39	0.15	0.19	0.20
Fe_{55}	0.43	0.12	0.17	0.18		
Fe_{147}	0.04	0.02	0.04	0.04		
Co_{13}	0.54	0.07	0.53	0.18	0.51	0.16
Co_{55}	0.61	0.14	0.23	0.04		
Co_{147}	0.11	0.03	0.14	0.02		
Ni_{13}	0.94	0.03	0.62	0.00	0.58	0.13
Ni_{55}	0.27	0.03	0.25	0.01		
Ni_{147}	0.14	0.00	0.10	0.02		

with respect to the total magnetic moment is searched using *ab initio* calculations based on spin-polarized density functional theory. It is found that icosahedral structures are lower in energy than other structures at all total magnetic moments. The cohesive energy of a cluster increases as size of cluster is increased. This is due the fact that surface energy of a surface in Fe, Co, and Ni is positive and consequently the surface energy tends to decrease the cohesive of a cluster. The surface to volume ratio decreases as size of cluster is increased and consequently the cohesive energy increases. As the size of cluster is increased, the nearest-neighbor bond length is increased toward bulk value. We find that the magnetic and electronic structures of a cluster are dependent on its size, intrastructure, and geometrical structure symmetries. The local magnetic moment of surface atom increases almost linearly while local magnetic moment of center atom increases nonmonotonically as total magnetic moment of cluster is increased. The M_{13} and M_{55} (M=Fe, Co, Ni) atomic clusters are half metallic in the sense that HOMO-LUMO energy gap is very small for minority spin as compared to that for majority-spin component. However, 147-atom clusters are metallic as the HOMO-LUMO energy gaps for both spin components are zero or nearly zero.

ACKNOWLEDGMENTS

This work is funded by the Deutsche Forschungsgemeinschaft (DFG) under Project No. Kr-1805/8-1 (SPP 1801). We also cordially acknowledge the CCC Aachen (SunFire), RWTH Aachen for providing computational facility.

*Present address: Max Planck Institute for Solid State Research, Heisenbergstrasse 1, Stuttgart, Germany.

[1] G. Schön and U. Simon, Colloid Polym. Sci. **273**, 101 (1995).
[2] G. Schmid, M. Bäumle, M. Geerkens, I. Heim, C. Osemann, and T. Sawitowski, Chem. Soc. Rev. **28**, 179 (1999).
[3] J. D. Aiken and R. G. Finke, J. Mol. Catal. Chem. **145**, 1 (1999).
[4] P. Migowski and J. Dupont, Chem. Eur. J. **13**, 32 (2007).
[5] U. Schubert, J. Sol-Gel Sci. Technol. **31**, 19 (2004).
[6] F. Stellacci, Nat. Mater. **4**, 113 (2005).
[7] J. Bansmann *et al.*, Surf. Sci. Rep. **56**, 189 (2005).
[8] F. Baletto and R. Ferrando, Rev. Mod. Phys. **77**, 371 (2005).
[9] A. D. Zdetsis, Rev. Adv. Mater. Sci. **11**, 56 (2006).
[10] M. Schmidt, R. Kusche, T. Hippler, J. Donges, W. Kronmüller, B. von Issendorff, and H. Haberland, Phys. Rev. Lett. **86**, 1191 (2001).
[11] S. H. Yang, D. A. Drabold, J. B. Adams, and A. Sachdev, Phys. Rev. B **47**, 1567 (1993).
[12] S. Debiaggi and A. Caro, Phys. Rev. B **46**, 7322 (1992).
[13] H. Lei, J. Phys.: Condens. Matter **13**, 3023 (2001).
[14] E. K. Parks, L. Zhu, J. Ho, and S. J. Riley, Z. Phys. D **26**, 41 (1993).
[15] Y. Teng, X. Zeng, H. Zhang, and D. Sun, J. Phys. Chem. B **111**, 2309 (2007).
[16] V. Kumar and Y. Kawazoe, Eur. Phys. J. D **24**, 81 (2003).
[17] W. C. Wang, Y. Kong, X. He, and B. X. Liu, Appl. Phys. Lett. **89**, 262511 (2006).
[18] I. M. L. Billas, A. Châtelain, and W. A. de Heer, J. Magn. Magn. Mater. **168**, 64 (1997).
[19] M. B. Knickelbein, J. Chem. Phys. **125**, 044308 (2006).
[20] I. M. L. Billas, J. A. Becker, A. Châtelain, and W. A. de Heer, Phys. Rev. Lett. **71**, 4067 (1993).
[21] S. E. Apsel, J. W. Emmert, J. Deng, and L. A. Bloomfield, Phys. Rev. Lett. **76**, 1441 (1996).
[22] X. Xu, S. Yin, R. Moro, and W. A. de Heer, Phys. Rev. Lett. **95**,

237209 (2005).
[23] S. Linderoth and S. N. Khanna, J. Magn. Magn. Mater. **104-107**, 1574 (1992).
[24] D. C. Douglass, A. J. Cox, J. P. Bucher, and L. A. Bloomfield, Phys. Rev. B **47**, 12874 (1993).
[25] J. P. Bucher, D. C. Douglass, and L. A. Bloomfield, Phys. Rev. Lett. **66**, 3052 (1991).
[26] E. K. Parks, B. J. Winter, T. D. Klots, and S. J. Riley, J. Chem. Phys. **96**, 8267 (1992).
[27] O. Diéguez, M. M. G. Alemany, C. Rey, P. Ordejón, and L. J. Gallego, Phys. Rev. B **63**, 205407 (2001).
[28] M. L. Tiago, Y. Zhou, M. M. G. Alemany, Y. Saad, and J. R. Chelikowsky, Phys. Rev. Lett. **97**, 147201 (2006).
[29] J. M. Montejano-Carrizales, M. P. Iniguez, J. A. Alonso, and M. J. López, Phys. Rev. B **54**, 5961 (1996).
[30] Z. Q. Li and B. L. Gu, Phys. Rev. B **47**, 13611 (1993).
[31] K. Miura, H. Kimura, and S. Imanaga, Phys. Rev. B **50**, 10335 (1994).
[32] J. L. Rodriguez-López, F. Aguilera-Granja, K. Michaelian, and A. Vega, Phys. Rev. B **67**, 174413 (2003).
[33] O. Šipr, M. Košuth, and H. Ebert, Phys. Rev. B **70**, 174423 (2004).
[34] S. Polesya, S. B. O. Šipr, J. Minár, and H. Ebert, Europhys. Lett. **74**, 1074 (2006).
[35] L.-L. Wang and D. D. Johnson, Phys. Rev. B **75**, 235405 (2007).
[36] C. D. Dong and X. G. Gong, Phys. Rev. B **78**, 020409(R) (2008).
[37] V. Kumar and Y. Kawazoe, Phys. Rev. B **77**, 205418 (2008).
[38] O. V. Salata, J. Nanobiotech. **2**, 3 (2004).
[39] E. Duguet, S. Vasseur, S. Mornet, and J. M. Devoisselle, Nanomedicine **1**, 157 (2006).
[40] C. Riviere, S. Roux, O. Tillement, C. Billotey, and P. Perriat, Ann. Chim. (Paris) **31**, 351 (2006).
[41] S. D. Bader, Rev. Mod. Phys. **78**, 1 (2006).
[42] C. Pecharroman, A. Esteban-Cubillo, I. Montero, J. S. Moya, E. Aguilar, J. Santaren, and A. Alvarez, J. Am. Ceram. Soc. **89**, 3043 (2006).
[43] J. P. Perdew, J. A. Chevary, S. H. Vosko, K. A. Jackson, M. R. Pederson, D. J. Singh, and C. Fiolhais, Phys. Rev. B **46**, 6671 (1992).
[44] G. Kresse and J. Furthmüller, Comput. Mater. Sci. **6**, 15 (1996).
[45] G. Kresse and J. Furthmüller, Phys. Rev. B **54**, 11169 (1996).
[46] P. E. Blöchl, Phys. Rev. B **50**, 17953 (1994).
[47] G. Kresse and D. Joubert, Phys. Rev. B **59**, 1758 (1999).
[48] G. Rollmann, P. Entel, and S. Sahoo, Comput. Mater. Sci. **35**, 275 (2006).
[49] C. Kittel, *Introduction to Solid State Physics*, 7th ed. (Wiley, New York, 1996).